MolecularMedicine

# Aspirin's Active Metabolite Salicylic Acid Targets High Mobility Group Box 1 to Modulate Inflammatory Responses

*Hyong Woo Choi,[1] Miaoying Tian,[1*†] Fei Song,[2*] Emilie Venereau,[4] Alessandro Preti,[4] Sang-Wook Park,[1‡] Keith Hamilton,[2] G V T Swapna,[2] Murli Manohar,[1] Magali Moreau,[1] Alessandra Agresti,[4] Andrea Gorzanelli,[4] Francesco De Marchis,[4] Huang Wang,[2] Marc Antonyak,[5] Robert J Micikas,[1] Daniel R Gentile,[1§] Richard A Cerione,[5] Frank C Schroeder,[1] Gaetano T Montelione,[2,3] Marco E Bianchi,[4] and Daniel F Klessig[1]*

[1]Boyce Thompson Institute for Plant Research, Ithaca, New York, United States of America; [2]Center of Advanced Biotechnology and Medicine, Department of Molecular Biology and Biochemistry, and Northeast Structural Genomics Consortium, Rutgers, The State University of New Jersey, Piscataway, New Jersey, United States of America; [3]Department of Biochemistry and Molecular Medicine, Robert Wood Johnson Medical School, Rutgers, The State University of New Jersey, Piscataway, New Jersey, United States of America; [4]Division of Genetics and Cell Biology, San Raffaele University and Research Institute, Milano, Italy; [5]Department of Chemistry and Chemical Biology, Department of Molecular Medicine, Cornell University, Ithaca, New York, United States of America; [†]current affiliation: Department of Plant and Environmental Protection Sciences, University of Hawaii at Manoa, Honolulu, Hawaii, United States of America; [‡]current affiliation: Department of Entomology and Plant Pathology, Auburn University, Auburn, Alabama, United States of America; and [§]current affiliation: Department of Cellular and Molecular Pharmacology, University of California San Francisco, San Francisco, California, United States of America

Salicylic acid (SA) and its derivatives have been used for millennia to reduce pain, fever and inflammation. In addition, prophylactic use of acetylsalicylic acid, commonly known as aspirin, reduces the risk of heart attack, stroke and certain cancers. Because aspirin is rapidly de-acetylated by esterases in human plasma, much of aspirin's bioactivity can be attributed to its primary metabolite, SA. Here we demonstrate that human high mobility group box 1 (HMGB1) is a novel SA-binding protein. SA-binding sites on HMGB1 were identified in the HMG-box domains by nuclear magnetic resonance (NMR) spectroscopic studies and confirmed by mutational analysis. Extracellular HMGB1 is a damage-associated molecular pattern molecule (DAMP), with multiple redox states. SA suppresses both the chemoattractant activity of fully reduced HMGB1 and the increased expression of proinflammatory cytokine genes and cyclooxygenase 2 (COX-2) induced by disulfide HMGB1. Natural and synthetic SA derivatives with greater potency for inhibition of HMGB1 were identified, providing proof-of-concept that new molecules with high efficacy against sterile inflammation are attainable. An HMGB1 protein mutated in one of the SA-binding sites identified by NMR chemical shift perturbation studies retained chemoattractant activity, but lost binding of and inhibition by SA and its derivatives, thereby firmly establishing that SA binding to HMGB1 directly suppresses its proinflammatory activities. Identification of HMGB1 as a pharmacological target of SA/aspirin provides new insights into the mechanisms of action of one of the world's longest and most used natural and synthetic drugs. It may also provide an explanation for the protective effects of low-dose aspirin usage.

**Online address: http://www.molmed.org**
**doi: 10.2119/molmed.2015.00148**

## INTRODUCTION

The plant-derived phenolic compound salicylic acid (SA) and its derivatives, known collectively as salicylates, have long been used to reduce pain, fever, and inflammation (1–3). Records from the third century B.C. indicate that Hippocrates prescribed willow bark and leaves, which contain salicylates, to relieve pain and fever (4). The best-known salicylate is acetylsalicylic acid, commonly known as aspirin. In addition to its antiinflammatory, antipyretic and analgesic effects (5–7), prophylactic use of aspirin reduces the risk of heart attack, stroke and certain cancers (3,8,9). Aspirin's primary mechanism of action in mammals has been attributed to disruption of eicosanoid biosynthesis through irreversible inhibition via acetylation of cyclooxygenases (COX) 1 and 2, thereby altering the levels of prostaglandins, hormones that are involved in inflammation

*These two authors contributed equally.
***Address correspondence to*** *Daniel F Klessig, Boyce Thompson Institute for Plant Research, Ithaca, NY 14853. Phone: 607-254-4560; Fax: 607-254-1242; E-mail: dfk8@cornell.edu; Marco E Bianchi, San Raffaele University and Research Institute, Milan, Italy. Phone: +39-02-2643-4765; Fax: +39-02-2643-5544; E-mail: bianchi.marco@hsr.it; Gaetano T Montelione, The State University of New Jersey, Piscataway NJ 08854. Phone: 732-235-5375; Fax: 732-235-5779; E-mail: guy@cabm.rutgers.edu.*
*Submitted June 17, 2015; Accepted for publication June 18, 2015; Published Online (www.molmed.org) June 18, 2015.*

and pain (7). Aspirin is rapidly deacetylated to SA by esterases in human plasma, with a half-life of conversion of 13–19.5 min (10). SA's half maximal inhibitory concentration ($IC_{50}$) for COX-2 enzymatic activity *in vitro* is much higher (>100 mg/L, or ~500 μmol/L) than aspirin's (6.3 mg/L, or ~35 μmol/L); yet SA and aspirin have largely the same pharmacological effects (7). Thus, aspirin/SA likely have additional mechanisms of action that are only partially understood.

In plants, SA is involved in many physiological processes, including immunity, where it plays a central role (3). To decipher SA's mechanisms of action, we have identified several plant SA-binding proteins (SABPs) (3,11,12). By applying the approaches developed for identifying plant SABPs to mammalian cells, we have discovered a new target of SA in humans, the high mobility group box 1 protein, HMGB1.

HMGB1 is an abundant, chromatin-associated protein that is present in all animal cells; fungi and plants have related proteins (13). Structurally, HMGB1 is composed of two basic DNA-binding domains, designated HMG boxes A and B, and a highly acidic C-terminal tail that participates in specific intramolecular interactions (14). In the nucleus, HMGB1 binds DNA to facilitate nucleosome formation and transcription factor binding (15). HMGB1 also acts as a DAMP molecule, with chemoattractant and cytokine-inducing activities upon its release into the extracellular milieu from necrotic, damaged or severely stressed cells (16).

Extracellular HMGB1 mediates a range of biological responses in association with multiple receptors, such as the receptor for advanced glycation end products (RAGE), Toll-like receptor 2 (TLR2), TLR4 and C-X-C chemokine receptor type 4 (CXCR4) (16). HMGB1 has multiple redox states, which in part depend on a reversible intramolecular disulfide bond formed between cysteine residues 23 and 45 (17). Disulfide HMGB1 signaling through TLR4 leads to activation of nuclaar factor kappa-B (NF-κB) and transcription of proinflammatory cytokines (17,18), whereas recognition by CXCR4 of a complex formed by fully reduced HMGB1 with the C-X-C motif chemokine 12 (CXCL12) promotes the recruitment of inflammatory cells to damaged tissue (19). HMGB1's diverse activities and receptors likely account for its multiple roles in human disease, including sepsis and arthritis (20,21), atherosclerotic plaque formation (22) and cancer (23–25). Consequently, HMGB1 has attracted considerable attention as an important drug target for various human diseases (13,16,20–25).

We show here that SA, as well as synthetic and natural SA derivatives, bind HMGB1 in two distinct binding sites and inhibit its extracellular chemoattractant and cytokine-inducing activities. Mutations in one of the SA-binding sites, which disrupt binding of SA and its derivatives, also suppress inhibition by SA and its derivatives of HMGB1's chemoattractant activity.

## MATERIALS AND METHODS

### Identification of SA-Binding Protein from HeLa Cells

Approximately $3.5 \times 10^7$ HeLa cells were trypsinized and pelleted after neutralization and resuspended in 2 mL of 0.2 mol/L Tris-HCl (pH 7.4) containing 137 mmol/L NaCl, 1 mmol/L EDTA, 0.5% (v/v) Triton X-100, 1 mmol/L phenylmethanesulfonylfluoride (PMSF) and a protease inhibitor cocktail (Sigma-Aldrich). The suspension was then subjected to two freeze–thaw cycles, and cells were disrupted by ultrasound. The solution was clarified by a 10-min spin at 20,000*g* and dialyzed against loading buffer, 50 mmol/L $KPO_4$ (pH 7.0) containing 50 mmol/L NaCl, a protease inhibitor cocktail (Sigma-Aldrich) and 0.1 % (v/v) Triton X-100.

The preparation of SA-immobilized resin and purification of SABPs with this resin were previously described (12). Three enriched proteins from the SA eluate were excised and subjected to electrospray ionization–tandem mass spectrometry (ESI-MS/MS) for peptide identification (Donald Danforth Plant Science Center, St Louis, MO, USA).

### Cloning, Expression, and Purification of HMGB1

The rat HMGB1 expression plasmid pET30 Xa/LIC HMGB1 was kindly provided by S Lippard (26). Because there are two amino acid differences between rat and human HMGB1, we generated a human HMGB1 expression clone, pET30 Xa/LIC hHMGB1, by introducing PCR-based point mutations that converted residues 189D and 202E to 189E and 202D. Box A (residues 10–80) and Box B (residues 96–164) domains were amplified from pET30 Xa/LIC HMGB1 and cloned into *Kpn*I and *Eco*RI sites of pET30 Xa/LIC. Recombinant human HMGB1, Box A and Box B proteins were expressed in *Escherichia coli* strain BL21 cells grown at 37°C to $OD_{600}$ = 0.7. HMGB1 expression was induced by adding 0.1 mmol/L isopropylthiogalactoside (IPTG) for 16 h at room temperature. Cells were collected by centrifugation at 6,000*g* for 30 min, and stored at –20°C. For protein purification, cells were resuspended in lysis buffer, buffer A (20 mmol/L Tris-HCl/8.0, 0.15 mol/L NaCl, 2 mmol/L β-mercaptoethanol and 10% glycerol) containing 0.2% NP-40, 1 mg/mL lysozyme, 1 mmol/L PMSF and 10 mmol/L imidazole. After sonication and centrifugation at 20,000*g* for 1 h, soluble 6xHis-tagged HMGB1 was purified by affinity chromatography using nickel nitrilotriacetic acid (Ni-NTA) agarose resin (Novagen); after washing the HMGB1-bound resin with buffer A containing 20 mmol/L imidazole, HMGB1 was eluted in buffer A containing 300 mmol/L imidazole. The 6xHis tag was removed by overnight incubation at 4°C with factor Xa (for full-length HMGB1) and thrombin (for Box A or Box B). The cleaved HMGB1 was further purified using gel filtration chromatography on a HiLoad 16/60 Superdex 200 column (GE Healthcare) equilibrated in buffer A.

To prepare fully reduced HMGB1, purified HMGB1 was incubated with 5 mmol/L dithiothreitol for 1 h at 4°C,

and then desalted using a PD-10 desalting column (GE Healthcare) equilibrated in 20 mmol/L Tris-HCl/8.0 and 20 mmol/L NaCl plus 0.5 mmol/L DTT. Disulfide HMGB1 was prepared in the absence of any reducing agent. Contaminating lipopolysaccharide (LPS) were removed from all HMGB1 preparations used for biological assays as described (17). For some experiments, fully reduced HMGB1 and disulfide HMGB1 were provided by HMGBiotech (Milan, Italy).

### SA-Binding Analyses

Analyses of candidate SABPs by photoaffinity labeling with 4-azido salicylic acid (4-AzSA) and by surface plasmon resonance (SPR) with 3-aminoethyl SA (3AESA) were previously described (11,12).

### NMR Sample Preparation

All four HMGB1 constructs (Box A, Box B, HMGB1-ΔC and full length HMGB1) were cloned in either pET15Tev_NESG or Avi-NESG expression vectors, which both include a Tomato Etch Virus proteas (TEV)-cleavable N-terminal 6xHis purification tag, expressed with uniform $^{15}N$ or $^{13}C$,$^{15}N$-enrichment, and purified using the published protocols of the Northeast Structural Genomics Consortium (NESG) (27,28). Protein constructs were purified with a 5-mL HisTrap HP Ni-NTA column (GE Healthcare), cleaved with TEV-protease, and repurified using a 5-mL HisTrap HP column. Size exclusion chromatography was performed using a HiLoad 26/600 Superdex 75 column (GE Healthcare) Q1 with a buffer containing 50 mmol/L Tris-HCl, pH 7.5, 100 mmol/L NaCl, 0.02% $NaN_3$, and 10 mmol/L DTT. Samples for nuclear magnetic resonance (NMR) studies were exchanged into this same buffer, containing either no SA, SA, amorfrutin B1 or ac3AESA using a Zeba 96-well spin-desalting plate (Thermo Scientific).

### NMR Data Collection

NMR samples (50–200 μL) contained 0.25 mmol/L protein in 20 mmol/L $NaPO_4$, pH 7.5, 100 mmol/L NaCl, 0.02% $NaN_3$ and 1 mmol/L tris(2-carboxyethyl)phosphine (TCEP). Samples were analyzed with and without SA or other candidate inhibitors at 25°C. Chemical shift perturbation studies were carried out using either a Bruker Avance 800-MHz NMR system with 4-mm NMR tubes or a Bruker Avance 600 MHz NMR spectrometer equipped with a 1.7-mm micro cryoprobe; 1024 or 2048 complex points were acquired for each of 80 to 200 increments in the $^{15}N$ dimension with a recycle delay of 1 s. Each spectrum was typically acquired for 2–8 h Composite changes in $^{1}H$ and $^{15}N$ backbone amide chemical shifts (29), $\Delta\delta_{(N-H)}$, were computed as:

$$\Delta\delta_{(N-H)} = \sqrt{(^{H}\Delta\delta_{ppm})^2 + (^{N}\Delta\delta_{ppm}/6)^2}$$

### Assays for Cytokine Induction

Total RNAs were isolated using the Illustra RNAspin Mini kit (GE Healthcare), and complementary DNAs (cDNAs) were obtained by reverse transcription with oligo(dT) primers (Invitrogen) and SuperScript II Reverse Transcriptase (Invitrogen) following the manufacturers' instructions. Quantitative real-time PCR was performed using a LightCycler480 (Roche Molecular Diagnostics), in duplicates, using SYBR Green I master mix. The ΔCt method was used for quantification, and the β-actin gene was used for normalization.

### Chemotaxis Assay

The downside of polyvinylpirrolidone (PVP)-free polycarbonate filters (8 μm pores; Millipore) was coated with 50 μg/mL fibronectin (Sigma-Aldrich). Serum-free Dulbecco modified Eagle medium (DMEM) (negative control), DMEM containing 0.1 nmol/L N-formyl-methionyl-leucyl-phenylalanine (fMLP) (positive control; Sigma-Aldrich), or DMEM containing 1 nmol/L fully reduced HMGB1 or disulfide HMGB1 were placed in the lower chamber, together with different concentrations of SA (Sigma-Aldrich). Mouse 3T3 fibroblasts were cultured in DMEM media supplemented with 10% fetal bovine serum (FBS) until 90% confluence, washed twice with phosphate-buffered saline (PBS) to eliminate any floating cells and harvested with trypsin. A total of 50,000 cells in 200 μL were added to the upper chamber, and cells were left to migrate for 3 h at 37°C. Nonmigrating cells were removed with a cotton swab, and migrated cells were fixed with ethanol and stained with Giemsa.

### Statistical Analysis

The results are expressed as a mean ± standard deviation (SD). Statistical analysis on the group differences was performed by using a Tukey honest significant difference (HSD) test with software JMP Pro, version 10.0.0 (SAS Institute Inc.).

*All supplementary materials are available online at www.molmed.org.*

## RESULTS

### Identification of HMGB1 as an SA-Binding Protein

To identify novel salicylate effectors and/or receptors, we subjected HeLa cell extracts to affinity chromatography on a PharmaLink column to which SA was linked. After stringent washing with the biologically inactive SA analog 4-hydroxy benzoic acid, the column was competitively eluted with SA (Figure 1A). The released proteins were analyzed by mass spectroscopy and HMGB1 (GI: 4504425) was repeatedly identified.

SA-binding activity of fully reduced HMGB1 was then assessed using photoaffinity crosslinking (11,12). Immunoblotting of 4-azido SA (4AzSA) crosslinked products with α-SA antibody revealed a band at the expected molecular weight for HMGB1 when 4AzSA was present in the reaction, but not in the control reaction without 4AzSA (Figure 1B). Increasing concentrations of SA inhibited crosslinking of

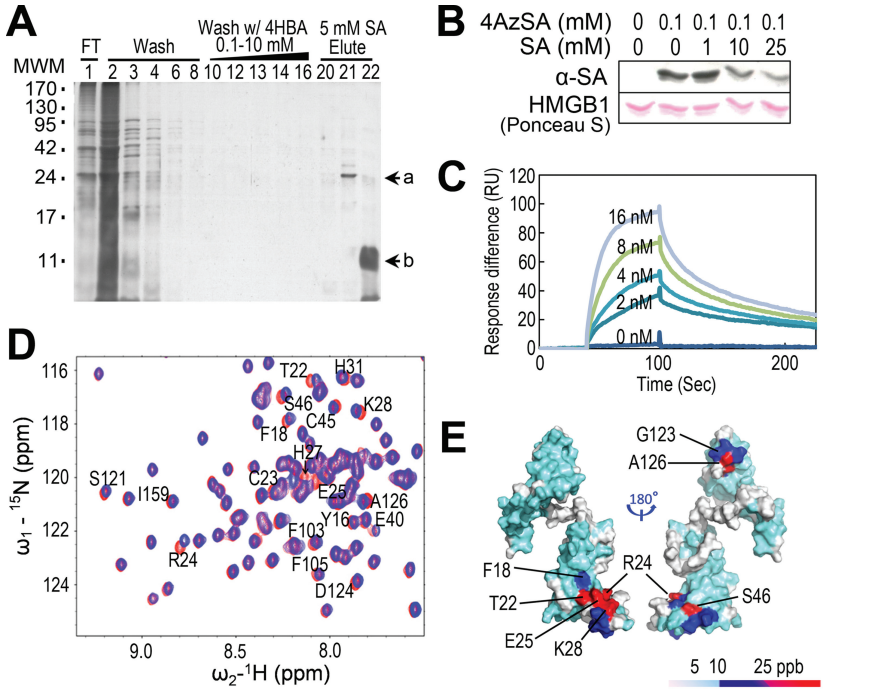


**Figure 1.** Identification of HMGB1 as an SA-binding protein and its SA-binding sites. (A) Affinity purification of SABPs from human HeLa cells. Total protein extracts prepared from human HeLa cells were chromatographed on an SA-immobilized PharmaLink column. After washing with increasing concentrations of the biologically inactive SA analog, 4-hydroxy benzoic acid (4-HBA), the retained proteins were eluted with 5 mmol/L SA, fractionated by gel electrophoresis and resolved by silver staining. Subsequent MS analyses identified band a as HMGB1 (GI: 4504425). Note that the band denoted by "b" was identified as soybean trypsin inhibitor, added to inhibit protein degradation. MWM, molecular weight markers. (B) Photoaffinity labeling of HMGB1 using 4AzSA. HMGB1 was incubated with or without 0.1 mmol/L 4AzSA in the absence or presence of the indicated concentrations of SA for 1 h, and then treated with UV light (50 mJ). Proteins labeled with 4AzSA were detected by immunoblot analysis with α-SA antibodies. Proteins stained with Ponceau S served as a loading control. (C) HMGB1 has strong affinity for 3AESA with an apparent $K_d$ of 1.48 nmol/L. Sensorgrams of concentration-dependent HMGB1 interacting with 3AESA immobilized on the SPR sensor chip. (D and E) Identification of SA binding sites on HMGB1. (D) $^{15}$N-$^{1}$H-HSQC spectra for HMGB1-ΔC were generated in the presence (blue) or absence (red) of 10 mmol/L SA; expanded regions of the spectra were then superimposed. Residues that show significant chemical shift perturbations (CSPs) due to SA binding are labeled. (E) SA-induced CSPs mapped onto the 3D structure of human HMGB1-ΔC (PDB id: 2YRQ, residues 6–164). The colors in the space-filling model correspond to the amplitude of the observed CSPs (cyan: $\Delta\delta_{(N-H)} < 12$ ppb; blue: $12 < \Delta\delta_{(N-H)} < 25$ ppb; red: $\Delta\delta_{(N-H)} > 25$ ppb, as indicated by the scale). Residues for which the backbone $^{15}$N-$^{1}$H resonance assignments are not available due to rapid exchange of surface amide protons and/or proline residues are shown in white.

4AzSA to fully reduced HMGB1, indicating that this interaction reflects authentic SA-binding activity. To further confirm HMGB1's SA-binding activity, we used surface plasmon resonance (SPR), which provides sensitive and quantitative measurements of bimolecular interactions in real-time (11). An SA derivative, 3-aminoethyl SA (3AESA), was synthesized and affixed to the CM5 sensor chip via an amide bond formed between the amine group of 3AESA and the carboxyl groups on the chip. The ethylamine group was added at the 3 position of the phenyl ring because several SA derivatives with substitutions at this position could still bind plant SABPs and induce immune responses (11) in plants. Binding was detected by flowing fully reduced HMGB1 over the 3AESA-immobilized sensor chip. A dose-dependent response was obtained with nmol/L concentrations of fully reduced HMGB1, indicating strong binding (Figure 1C).

### Characterization of SA-Binding Sites in HMGB1

To identify which domain(s) of HMGB1 binds SA, four constructs were generated: (i) full-length (FL): residues 1–215, (ii) HMGB1-ΔC: residues 1–165, (iii) Box A: residues 8–78, and (iv) Box B: residues 86–165 (Supplementary Figure S1A). SPR analysis revealed that all four constructs exhibited SA-binding activity, indicating that Box A and Box B both have an SA-binding site (Supplementary Figure S1B, C).

The amino acid (aa) residues in fully reduced HMGB1 affected by binding of SA were identified by $^{15}$N-$^{1}$H heteronuclear single quantum correlation (HSQC) 2D NMR spectroscopy at pH 7.5. Under these conditions, some surface amide protons are broadened due to solvent exchange, and cannot be observed. The sequence-specific resonance assignments for all observable backbone amide $^{15}$N and $^{1}H^{N}$ resonances of HMGB1-ΔC were determined using standard triple-resonance NMR methods (30,31). A region of the superimposed $^{15}$N-$^{1}$H-HSQC spectra obtained in the presence or absence of 10 mmol/L SA is shown in Figure 1D. Analysis of $^{15}$N-$^{1}$H HSQC spectra from HMGB1-ΔC showed that some backbone amide $^{1}H^{N}$ and/or N resonances exhibited significant chemical shift perturbations (CSPs) upon SA binding, including those of residues Phe18, Thr22, Arg24, Glu25, His27, Lys28, Glu40, Cys45 and Ser46 in Box A and Phe103, Ser121, Gly123, Asp124 and Ala126 in Box B. Similar re-

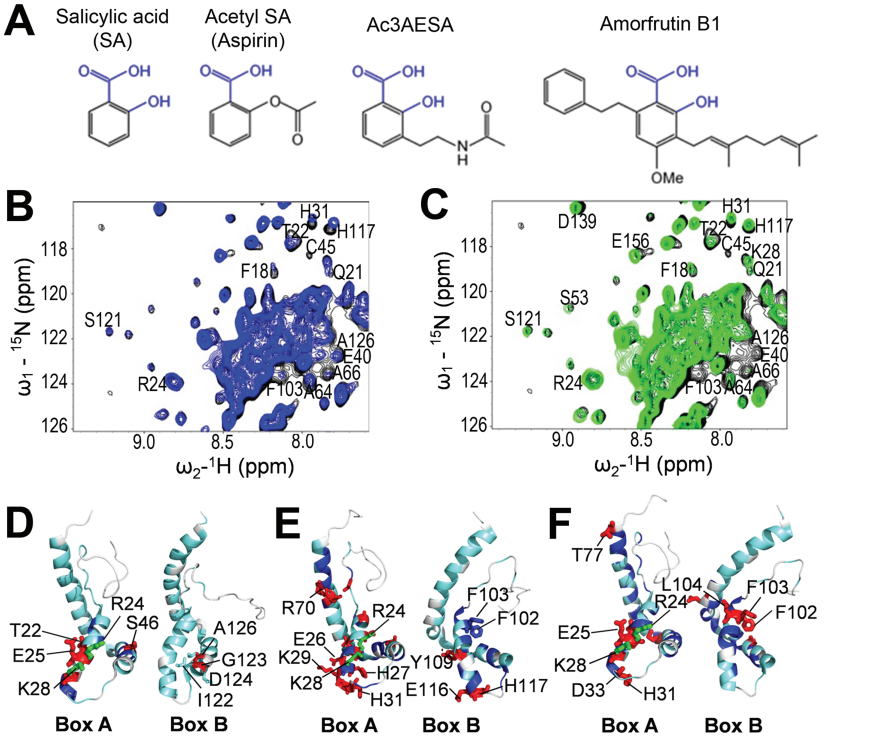


**Figure 2.** Ac3AESA and amorfrutin B1 bind in the SA-binding sites of HMGB1. (A) Chemical structures of SA and its synthetic and natural derivatives. Conserved hydroxyl (-OH) and carboxyl (-COOH) groups of salicylates are shown in blue. (B and C) 2D $^{15}$N-$^1$H HSQC spectra for full-length (FL) HMGB1. Spectra were recorded in the absence (black) or presence of 3 mmol/L ac3AESA (blue) (B) or 2 mmol/L amorfrutin B1 (green) (C). Expanded regions of the spectra were then superimposed. Residues that show significant CSPs due to ligand binding are labeled. (D–F) $^{15}$N-$^1$H $\Delta\delta_{(N-H)}$ CSPs due to SA (D), ac3AESA (E), and amorfrutin B1 (F) binding are mapped onto the 3D structure of human HMGB1 (PDB id: 2YRQ, residues 6–164), which is oriented to highlight the similarities and differences in the SA-binding sites of Box A and Box B. The colors correspond to the amplitude of the observed CSPs (cyan: $\Delta\delta_{(N-H)} < 12$ ppb; blue: $12 < \Delta\delta_{(N-H)} < 25$ ppb; red: $\Delta\delta_{(N-H)} > 25$ ppb); residues that both exhibit significant $\Delta\delta_{(N-H)}$ CSPs and were mutated to Ala are shown in green.

sults were obtained using Box A or Box B alone (Supplementary Figures S1D, E), confirming that both have SA-binding sites. The Box A and Box B domains of HMGB1 are structurally similar, and the CSPs due to SA binding are localized in corresponding regions of the two HMG-box domains (Figure 1E).

### Synthetic and Natural SA Derivatives Bind to HMGB1 with Higher Affinity than SA

Dissociation constants ($K_d$) derived by titrating with SA either Box A or FL HMGB1 suggested a $K_d$ in the range of 1 to 10 mmol/L. In contrast, fully reduced HMGB1 bound to 3AESA immobilized on the SPR sensor chip with much higher affinity, with an apparent $K_d$ in the nmol/L range (Figure 1C). SA crosslinking to the PharmaLink column involves a Mannich reaction, which adds an alkyl group to SA's phenyl ring. Likewise, 3AESA has an alkyl group on the phenyl ring. This suggests that SA derivatives containing alkyl groups are better ligands than SA. To test this possibility, the SA derivative acetyl-3AESA (ac3AESA) was synthesized from 3AESA by converting the charged amino moiety to a neutral acetylated amide, to resemble 3AESA linked to the SPR chip (Figure 2A). In addition, we identified natural SA derivatives, the amorfrutins, from the medicinal legume licorice *Glycyrrhiza foetida*, which also contains glycyrrhizin, a known inhibitor of HMGB1 (32,33). Amorfrutins have potent antidiabetic activity, which was ascribed to their ability to bind and activate peroxisome proliferator-activated receptor γ (34). Amorfrutins contain a phenyl ring with free carboxyl and hydroxyl groups at positions 1 and 2, respectively (Figure 2A). This is the SA core, which we have found to be critical for biological activity of SA derivatives in plants.

Comparison of the NMR spectra of FL HMGB1 in the absence versus presence of 15 mmol/L SA, 3 mmol/L ac3AESA, or 2 mmol/L amorfrutin B1 identified aa residues with significant CSPs in the presence of these compounds (Figures 2B, C and Supplementary Figure S2A–C). Mapping the ac3AESA- and amorfrutin B1-induced NMR CSPs onto the 3D structure of human HMGB1 published in the Protein Data Bank (PDB id: 2YRQ, residues 6–164) confirmed that SA, ac3AESA, and amorfrutin B1 share the same binding sites in Box A and Box B domains of the FL protein (Figures 2D–F). Furthermore, saturation transfer difference (STD) analysis (35), which detects magnetization transfer from a protein to its bound ligand, showed that ac3AESA is bound much more tightly than SA by HMGB1 (Supplementary Figure S3). At a ligand concentration of 6 mmol/L, no STD signal was detected for SA binding to FL HMGB1 (Supplementary Figure S3A), whereas significant STD signal was observed for ac3AESA at concentrations of 0.6–5.8 mmol/L (Supplementary Figure S3B).

Finally, we wished to test whether the free hydroxyl group at position 2 of the salicylate moiety is important for binding to HMGB1. WaterLogsy ligand detection experiments clearly show resonance transfer to SA, but no resonance

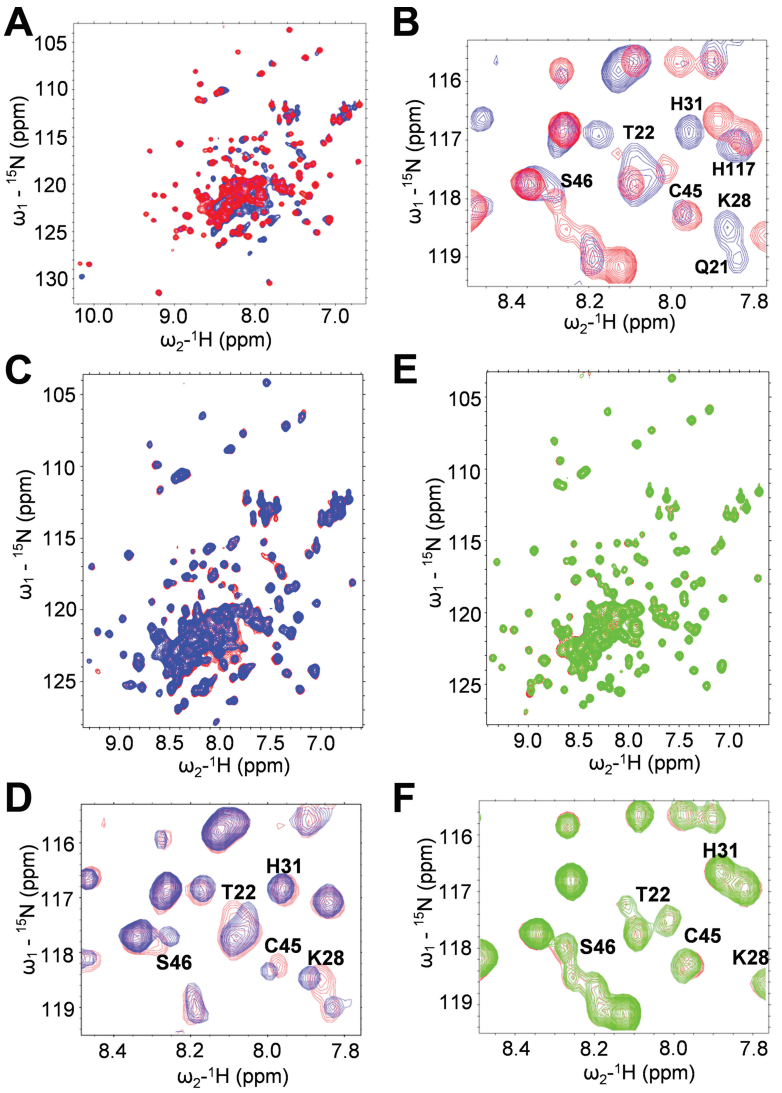


**Figure 3.** Arg24 and Lys28 are required for binding SA. (A and B) Comparison of 3D structure of WT versus R24A/K28A mutant FL HMGB1 by $^{15}$N-$^{1}$H HSQC 2D NMR spectroscopy. (A) R24A/K28A has a 3D structure similar to the WT HMGB1. This is demonstrated by superimposed $^{15}$N-$^{1}$H HSQC spectra of WT HMGB1 (blue) and of R24A/K28A (red). Most NH sites exhibit little or no CSP due to this double mutation. (B) Amide NHs that show significant CSPs in R24A/K28A (red) compared with the WT (blue) are all localized in or near the SA-binding sites in both Box A and Box B of FL HMGB1 and include many of the NH sites that exhibit CSP due to SA binding, which are labeled in this expanded region of the superimposed spectra. (C–F) Mutant HMGB1 does not bind SA. (C) $^{15}$N-$^{1}$H HSQC spectra for FL WT HMGB1 (~0.1 mmol/L) were generated in the presence (blue) or absence (red) of 15 mmol/L SA. (D) Residues that show significant CSPs due to SA binding are labeled in expanded regions of the superimposed spectra. (E) $^{15}$N-$^{1}$H HSQC spectra for R24A/K28A (~0.1 mmol/L) were generated in the presence (green) or absence (red) of 15 mmol/L SA. (F) Residues that show significant CSPs due to SA binding of WT, but not of R24A/K28A, are labeled in the expanded regions of the superimposed spectra.

transfer to aspirin (where the 2-OH group is acetylated) nor to 4-HBA (where the hydroxyl group in is in position 4 instead of 2) (Supplementary Figure S4). Likewise, $^{15}$N-$^{1}$H HSQC 2D NMR spectroscopy indicates that SA, but neither aspirin nor 4-HBA, binds HMGB1 (Supplementary Figure S5).

### Identification of an HMGB1 Mutant Unable to Bind SA or Its Derivatives

To confirm the identity of the SA-binding site, we mutated potentially key residues in HMGB1's Box A domain, including Arg24 and Lys28, which undergo CSPs in the presence of SA, ac3AESA, and amorfrutin B1. Because modeling (36) suggests that these residues form hydrogen bonds with SA and its derivatives, they were mutated to Ala to form the double mutant Arg24Ala/Lys28Ala (R24A/K28A). NMR analysis revealed that R24A/K28A mutant HMGB1 has a similar $^{15}$N-$^{1}$H HSQC spectrum as wild-type (WT) HMGB1, with small changes in chemical shifts localized mostly to residues near the mutation sites. Thus, this mutant protein appears to be folded properly (Figures 3A, B). Neither the presence of SA (Figures 3C–F), nor that of its two derivatives (Supplementary Figures S6A–D and S7A–D), induced CSPs in the residues of R24A/K28A HMGB1's Box A domain. Thus, R24A/K28A HMGB1 has lost SA-binding activity in its Box A domain.

### SA and Its Derivatives Inhibit the Chemoattractant Activity of HMGB1

Fully reduced HMGB1 forms a complex with the chemokine CXCL12 (19), which acts as a chemoattractant by binding to and activating the CXCR4 receptor. Thus, fully reduced HMGB1 mediates the migration of several cell types, including monocytes, fibroblasts, mesoangioblasts, smooth muscle cell, and cancer cells (17). Using a chemotaxis assay with mouse 3T3 fibroblasts, we tested whether SA and/or its derivatives alter HMGB1's chemoattractant activity. SA strongly inhibited HMGB1-elicited migration of fibroblasts in a dose-dependent manner, with an $IC_{50}$ of approximately 3-4 μmol/L (Figure 4A). By contrast, SA did not affect fibroblast migration induced by the well-known chemoattractant fMLP. Thus, SA appears to specifically inhibit HMGB1-

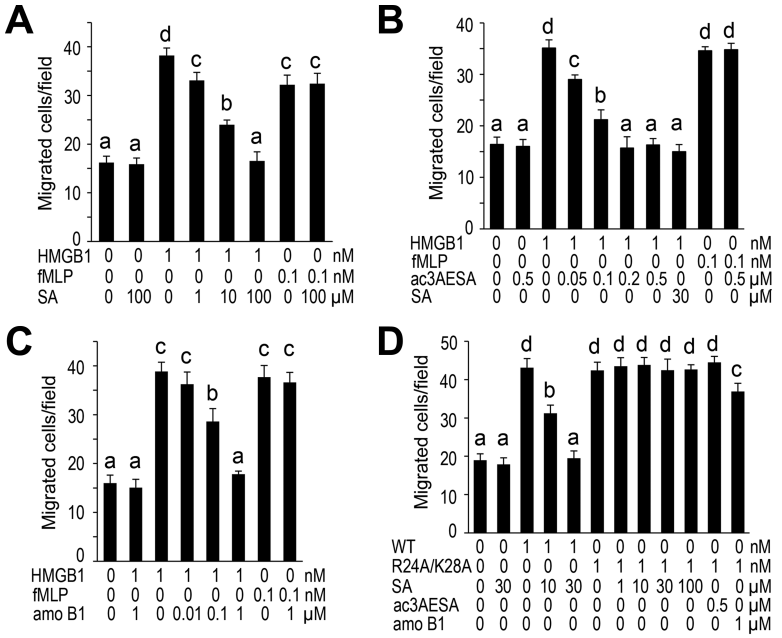


**Figure 4.** SA specifically inhibits fully reduced HMGB1's chemoattractant activity. (A–C) Dose-dependent inhibition of HMGB1's chemoattractant activity by SA (A), ac3AESA (B) and amorfrutin B1 (amo B1) (C). Migration of mouse 3T3 fibroblasts in the presence of 1 nmol/L fully reduced HMGB1, but not of 0.1 nmol/L fMLP, was blocked by indicated concentrations of SA, ac3AESA and amo B1. (D) Arg24 and Lys28 are required for binding SA and its derivatives and for their inhibition of HMGB1's chemoattractant activity by SA, ac3AESA and amo B1. The data represent the mean ± SD (n = 3). Means that are statistically different (Tukey HSD test, $P < 0.05$) are indicated by different letters over the bar. Means that are not statistically different are indicated by the same letter.

elicited migration, rather than suppress all cell migration per se. 4-HBA was ineffective in inhibiting migration (not shown), whereas aspirin could not be analyzed because it was readily hydrolyzed to SA during the experiment (not shown). The two SA derivatives also were found to suppress HMGB1's chemoattractant activity (Figure 4B, C): Ac3AESA was 40–60 times ($IC_{50}$ of ~70 nmol/L) more potent than SA, while amorfrutin B1 was ~50–70 times ($IC_{50}$ of ~60 nmol/L) more potent. Together these results suggest that synthetic and natural SA derivatives containing an additional alkyl group at position 3 bind more tightly to HMGB1 than SA, and as a result are more potent inhibitors.

Analysis of the R24A/K28A HMGB1 mutant revealed that it retained its chemoattractant activity which could no longer be inhibited by SA or its more potent derivatives (Figure 4D). This finding is consistent with its inability to bind these compounds (Supplementary Figures S6A–D and S7A–D).

Two more Box A double mutants were constructed—H27A/R48A and K12A/K68A. K12A/K68A retained SA-inhibitable chemoattractant activity (Supplementary Figure S8), demonstrating that only specific mutations in Box A disrupt SA binding and inhibition of HMGB1's chemoattractant activity. Mutant H27A/R48A no longer had chemoattractant activity, thus SA's effect on this activity could not be tested (Supplementary Figure S8).

The fact that a mutation that disrupts SA binding to the Box A domain of HMGB1 in NMR studies also abrogates SA inhibition of chemoattractant activity demonstrates that a site identified by NMR studies is functional in SA regulation of HMGB1's chemoattractant activity and strongly argues that SA directly affects HMGB1's proinflammatory activity.

### SA and ac3AESA Suppress Disulfide HMGB1's Induction of *PTGS2* and Cytokine Genes

Disulfide HMGB1 interacts with the myeloid differentiation factor 2 (MD-2) subunit of the TLR4 receptor and activates NF-κB–driven transcription of proinflammatory cytokine genes (17,18). Disulfide HMGB1 exhibited strong binding to immobilized 3AESA in our SPR analysis (Supplementary Figure S9). Because LPS interaction with MD-2/TLR4 induces the expression of the *PTGS2* gene (coding for the COX-2 enzyme, which is inducible) (37,38), we tested whether disulfide HMGB1 induces *PTGS2* expression. Indeed, disulfide HMGB1 induced *PTGS2* expression in human macrophages, along with that of classical inflammatory cytokine genes *IL6* and *TNF* (Figure 5A). SA and ac3AESA strongly inhibited induction of these genes by disulfide HMGB1 but had no effect in the absence of disulfide HMGB1 (Figure 5B). Notably, ac3AESA was efficient at concentrations 100-fold lower than that of SA (Figure 5B). In contrast, SA and ac3AESA did not suppress LPS-induced expression of these genes, but rather enhanced it slightly (Figure 5B), indicating that these salicylates specifically inhibit the cytokine-inducing activity of disulfide HMGB1, rather than suppressing all cytokine induction per se.

## DISCUSSION

Although SA and aspirin are widely used as nonsteroidal antiinflammatory drugs, their cellular targets and mechanisms of action are still being discovered. In this study, we identified HMGB1 as a novel SA-binding protein from HeLa cell extracts using affinity chromatography. Photoaffinity labeling,

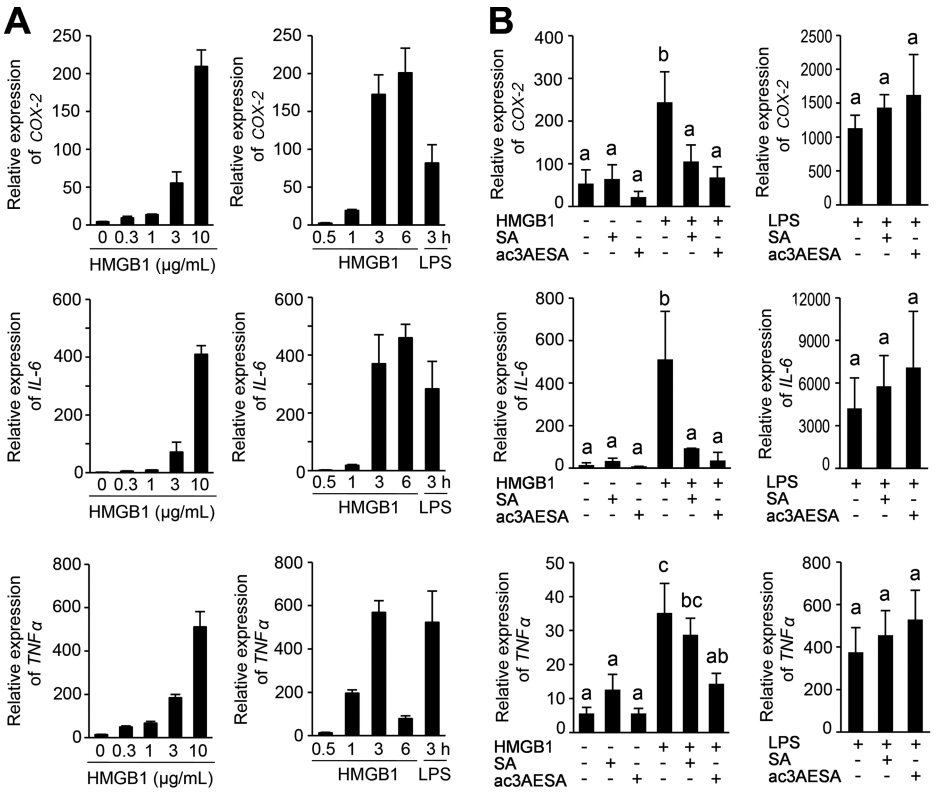


**Figure 5.** Effects of salicylates on disulfide HMGB1's cytokine-inducing activities in human macrophages. (A) Dose-dependent (left panels) and time-course (right panels) expression of *PTGS2* gene (coding for COX-2) and inflammatory cytokine genes (*IL6* and *TNF*) by following exposure to disulfide HMGB1. For the dose-effect experiment, macrophages were activated for 3 h with the indicated concentrations of HMGB1. For the time-course experiment, 10 μg/mL HMGB1 (~300 nmol/L) or 10 ng/mL LPS were used. (B) Inhibition of the cytokine-inducing activity of HMGB1, but not of LPS, by SA and ac3AESA. Human macrophages were activated for 3 h with 1 μg/mL HMGB1 (~30 nmol/L) (left panels) or 10 ng/mL LPS (right panels) in the absence or presence of 100 μmol/L SA or 1 μmol/L ac3AESA. The data are the mean ± SD (n = 3). Means that are statistically different (Tukey HSD test, $P < 0.05$) are indicated by different letters over the bar. Means that are not statistically different are indicated by the same letter.

SPR, and NMR analyses confirmed SA binding to HMGB1. NMR analyses revealed that CSPs upon SA binding are localized to residues in the HMG-box domains of both Box A and Box B. The SA-binding site in Box A identified by these NMR studies was confirmed by demonstrating that conversion of Arg24 and Lys28 to Ala did not affect HMGB1 folding or chemoattractant activity, but suppressed binding by SA and its two more potent derivatives and abrogated SA inhibition of its chemoattractant activity.

Despite weak binding of SA to HMGB1 in the conditions used for NMR experiments, SA inhibited the proinflammatory activities of HMGB1 at low μmol/L concentrations. We speculate that *in vivo* the conformation of HMGB1 is modified by the interaction with another molecule, so that the binding of salicylates is facilitated. Whereas this "missing molecule" has yet to be identified, several lines of evidence show that SA's effects on cells are due to direct interaction of SA with HMGB1. First, SA, but neither aspirin nor 4-HBA, binds HMGB1. Conversion of the hydroxyl of SA to an acetyl group (aspirin) or altering the position of the hydroxyl group on the phenyl ring (4-HBA) compromised HMGB1 binding. In contrast, ac3AESA and amorfrutin B1, which have additional groups on position 3, 4 or 6, were bound by HMBG1. These findings suggest that the SA core (free carboxyl and hydroxyl groups at position 1 and 2 of the phenyl ring) is critical for specific binding with HMGB1. Second, the SA derivative ac3AESA binds in HMGB1's SA-binding sites more tightly than SA and is a stronger inhibitor of its proinflammatory activities. Third, the binding sites for glycyrrhizin, a known HMGB1 inhibitor (32), and SA overlap (Supplementary Figure S10). Finally and most importantly, a mutant protein with alterations in the SA-binding site not only failed to bind SA and its more potent derivatives, but also failed to exhibit inhibition of its chemoattractant activity by SA and these derivatives. These results further confirm the identity of the SA-binding site and the direct effect SA exerts on the immune-related activities of HMGB proteins.

Moreover, we found that SA suppresses both HMGB1's proinflammatory activities, as it inhibits cell migration required for the recruitment of inflammatory cells, and the activation of the MD-2/TLR4 receptor for induction of cytokine and *PTGS2* gene expression (Figure 6). The concentration of SA in human plasma reaches ~140 μmol/L (~20 mg/L) within 1 h after intake of 500 mg of aspirin (39). This concentration should effectively inhibit HMGB1-induced chemotaxis, because it is far above the $IC_{50}$ (3–4 μmol/L or 0.45–0.6 mg/L), as well as the cytokine-inducing effect of disulfide HMGB1, which was strongly inhibited by 100 μmol/L SA. Notably, SA inhibits HMGB1's chemoattractant and cytokine-inducing activities, as well as the expression of the *PTGS2* gene coding for COX-2, at concentrations 10- to 50-fold below that required to inhibit COX-2's enzymatic activity *in vitro* (40). Thus, SA

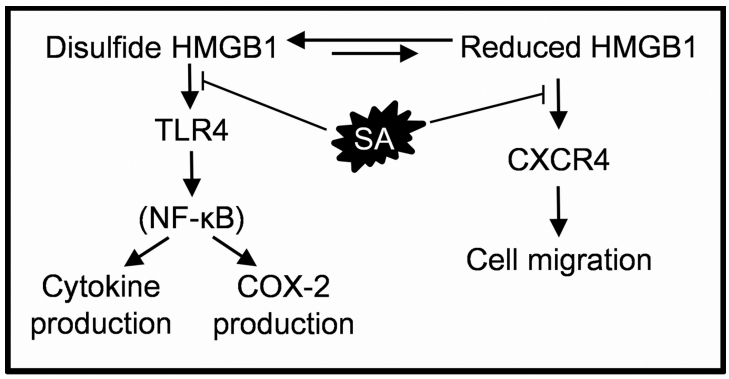


**Figure 6.** Schematic representation of SA's mechanisms of suppression of HMGB1's proinflammatory activities. Extracellular HMGB1 is recognized by two different receptors, CXCR4 and TLR4 (16). The fully reduced HMGB1 induces CXCR4-mediated cell migration. SA inhibits cell migration induced by HMGB1. The disulfide HMGB1 induces TLR4-mediated activation of the NF-κB signaling pathway (16,17), resulting in transcriptional activation of genes coding for COX-2 (*PTGS2*) and proinflammatory cytokines (*IL6* and *TNF*). SA suppresses disulfide HMGB1-induced *PTGS2*, *IL6* and *TNF* expression.

is one of the most potent inhibitors of HMGB1 described so far, and it interferes with both redox forms, contrary to other widely used inhibitors, which inhibit only its chemoattractant activity, such as some antibodies to HMGB1 (17).

Of particular note is the fact that SA targets a DAMP, which provides a new mechanism to explain the efficiency of aspirin in limiting sterile inflammation. Notably, SA did not suppress migration of cells to fMLP, which mimics N-formylated peptides characteristic of bacteria, or the induction of proinflammatory cytokines or COX-2 in macrophages exposed to LPS. Thus, SA might preferentially suppress sterile inflammation over pathogen-initiated inflammation. This is desirable because clinical management of injury requires specific attenuation of sterile inflammation, without compromising innate immunity against pathogens. Likewise, SA inhibits the cancer-promoting activities of HMGB1 in mesothelioma, whose cells are addicted to HMGB1 for growth and survival (41).

The identification of HMGB1 as another pharmacological target of SA/aspirin provides new insights into the mechanisms of action of the most widely used drug for reducing inflammation and inflammation-associated diseases. Moreover, together the identification of HMGB1's SA-binding sites by both NMR and site-directed mutagenesis and the discovery of natural and synthetic SA derivatives with greatly enhanced potency compared with SA in suppressing HMGB1's proinflammatory activities hold great promise for the development of improved SA-based drugs.

## ACKNOWLEDGMENTS

This work was supported by grants from (i) the Arabidopsis 2010 Initiative of the National Science Foundation USA (IOS-0820405 to DF Klessig ), (ii) the Protein Structure Initiative of the National Institutes of Health USA (NIH; U54-GM094597 to GT Montelione ), (iii) NIH (GM040654 to RA Cerione ), the Triad Foundation (to FC Schroeder ), and (iv) Associazione Italiana Ricerca sul Cancro (IG-14233 to ME Bianchi).

## DISCLOSURE

Several of the authors (DF Klessig, S-W Park, HW Choi, FC Schroeder, GT Montelione, K Hamilton, F Song, ME Bianchi) have applied for a patent based in part on the work described within. This does not alter our adherence to all *Molecular Medicine* policies on sharing data and materials.

## REFERENCES

1. Vane J. (1971) Inhibition of prostaglandin synthesis as a mechanism of action for aspirin-like drugs. *Nat. New Biol.* 231:232–5.
2. Weissmann G. (1991) Aspirin. *Sci. Am.* 264:84–90.
3. Vlot AC, Dempsey DA, Klessig DF. (2009) Salicylic Acid, a multifaceted hormone to combat disease. *Annu. Rev. Phytopathol.* 47:177–206.
4. Aboelsoud N. (2010) Herbal medicine in ancient Egypt. *J. Med. Plants Res.* 4:82–6.
5. Mitchell AG, Broadhead JF. (1967) Hydrolysis of solubilized aspirin. *J. Pharm. Sci.* 56:1261–6.
6. Rowland PM, Riegelman S, Harris PA, Sholkoff SD, Eyring EJ. (1967) Kinetics of acetylsalicylic acid disposition in man. *Nature* 215:413–4.
7. Ekinci D. (2011) Salicylic acid derivatives: synthesis, features and usage as therapeutic tools. *Expert Opin. Ther. Pat.* 21:1831–41.
8. Rothwell PM, *et al.* (2010) Long-term effect of aspirin on colorectal cancer incidence and mortality: 20-year follow-up of five randomised trials. *Lancet.* 376:1741–50.
9. Armitage J, *et al.* (2012) Aspirin for the older person: report of a meeting at the Royal Society of Medicine, London, 3rd November 2011. *Ecancermedicalscience.* 6:245.
10. Costello PB, Caruana JA, Green FA. (1984) The relative roles of hydrolases of the erythrocyte and other tissues in controlling aspirin survival *in vivo*. *Arthritis Rheum.* 27:422–6.
11. Tian M, *et al.* (2012) The combined use of photoaffinity labeling and surface plasmon resonance-based technology identifies multiple salicylic acid-binding proteins. *Plant J.* 72:1027–38.
12. Manohar M, *et al.* (2015) Identification of multiple salicylic acid-binding proteins using two high throughput screens. *Front. Plant Sci.* 5:777.
13. Lotze MT, Tracey KJ. (2005) High-mobility group box 1 protein (HMGB1): nuclear weapon in the immune arsenal. *Nat. Rev. Immunol.* 5:331–42.
14. Stott K, Watson M, Howe FS, Grossmann JG, Thomas JO. (2010) Tail-mediated collapse of HMGB1 is dynamic and occurs via differential binding of the acidic tail to the A and B domains. *J. Mol. Biol.* 403:706–22.
15. Celona B, *et al.* (2011) Substantial histone reduction modulates genomewide nucleosomal occupancy and global transcriptional output. *PLoS Biol.* 9:e1001086.
16. Andersson U, Tracey KJ. (2011) HMGB1 is a therapeutic target for sterile inflammation and infection. *Annu. Rev. Immunol.* 29:139–62.
17. Venereau E, *et al.* (2012) Mutually exclusive redox forms of HMGB1 promote cell recruitment or proinflammatory cytokine release. *J. Exp. Med.* 209:1519–28.
18. Yang H, *et al.* (2015) MD-2 is required for disul-

fide HMGB1-dependent TLR4 signaling. *J. Exp. Med.* 212:5–14.
19. Schiraldi M, *et al.* (2012) HMGB1 promotes recruitment of inflammatory cells to damaged tissues by forming a complex with CXCL12 and signaling via CXCR4. *J. Exp. Med.* 209:551–63.
20. Yang H, Ochani M, Li J. (2004) Reversing established sepsis with antagonists of endogenous high-mobility group box 1. *Proc. Natl. Acad. Sci. U. S. A.* 101:296–301.
21. Schierbeck H, *et al.* (2011) Monoclonal anti-HMGB1 (high mobility group box chromosomal protein 1) antibody protection in two experimental arthritis models. *Mol. Med.* 17:1039–44.
22. Porto A, *et al.* (2006) Smooth muscle cells in human atherosclerotic plaques secrete and proliferate in response to high mobility group box 1 protein. *FASEB J.* 20:2565–6.
23. Choi YR, *et al.* (2003) Overexpression of high mobility group box 1 in gastrointestinal stromal tumors with KIT mutation. *Cancer Res.* 63:2188–93.
24. Tang D, Kang R, Zeh HJ, Lotze MT. (2010) High-mobility group box 1 and cancer. *Biochim. Biophys. Acta.* 1799:131–40.
25. Jube S, *et al.* (2012) Cancer cell secretion of the DAMP protein HMGB1 supports progression in malignant mesothelioma. *Cancer Res.* 72:3290–301.
26. Ohndorf U, Rould M, He Q, Pabo C, Lippard S. (1999) Basis for recognition of cisplatin-modified DNA by high-mobility-group proteins. *Nature.* 399:708–12.
27. Xiao R, *et al.* (2010) The high-throughput protein sample production platform of the Northeast Structural Genomics Consortium. *J. Struct. Biol.* 172:21–33.
28. Acton TB, *et al.* (2011) Preparation of protein samples for NMR structure, function, and small-molecule screening studies. *Methods Enzymol.* 493:21–60.
29. Farmer B 2nd, *et al.* (1996) Localizing the NADP+ binding site on the MurB enzyme by NMR. *Nat. Struct. Biol* 3:995–7.
30. Biamonti C, Rios C, Lyons B, Montelione G. (1994) Multidimensional NMR experiments and analysis techniques for determining homo- and heteronuclear scalar coupling constants in proteins and nucleic acids. *Adv. Biophys. Chem.* 4:51–120.
31. Moseley HNB, Monleon D, Montelione GT. (2001) Automatic determination of protein backbone resonance assignments from triple resonance nuclear magnetic resonance data. *Methods Enzymol.* 339:91–108.
32. Mollica L, *et al.* (2007) Glycyrrhizin binds to high-mobility group box 1 protein and inhibits its cytokine activities. *Chem. Biol.* 14:431–41.
33. Sitia G, Iannacone M, Müller S, Bianchi ME, Guidotti LG. (2007) Treatment with HMGB1 inhibitors diminishes CTL-induced liver disease in HBV transgenic mice. *J. Leukoc. Biol.* 81:100–7.
34. Weidner C, *et al.* (2012) Amorfrutins are potent antidiabetic dietary natural products. *Proc. Natl. Acad. Sci. U. S. A.* 109:7257–62.
35. Mayer M, Meyer B. (2001) Group epitope mapping by saturation transfer difference NMR to identify segments of a ligand in direct contact with a protein receptor. *J. Am. Chem. Soc.* 123:6108–17.
36. Grosdidier A, Zoete V, Michielin O. (2011) SwissDock, a protein-small molecule docking web service based on EADock DSS. *Nucleic Acids Res.* 39:W270–7.
37. Silver RM, *et al.* (1995) Bacterial lipopolysaccharide-mediated fetal death. Production of a newly recognized form of inducible cyclooxygenase (COX-2) in murine decidua in response to lipopolysaccharide. *J. Clin. Invest.* 95:725–31.
38. Hwang D. (2001) Modulation of the expression of cyclooxygenase-2 by fatty acids mediated through toll-like receptor 4-derived signaling pathways. *FASEB J.* 15:2556–64.
39. Proost J, Imhoff G Van, Wesseling H. (1983) Plasma levels of acetylsalicylic acid and salicylic acid after oral ingestion of plain and buffered acetylsalicylic acid in relation to bleeding time and thrombocyte function. *Pharm. Weekbl. Sci.* 5:22–7.
40. Mitchell JA, Saunders M, Barnes PJ, Newton R, Belvisi MG. (1997) Sodium salicylate inhibits cyclo-oxygenase-2 activity independently of transcription factor (nuclear factor κB) activation: role of arachidonic acid. *Mol. Pharmacol.* 912:907–12.
41. Yang H, *et al.* (2015) Aspirin delays mesothelioma growth by inhibiting HMGB1-mediated tumor progression. *Cell Death Dis.* 6:e1786.

Cite this article as: Choi HW, *et al*. (2015) Aspirin's active metabolite salicylic acid targets high mobility group box 1 to modulate inflammatory responses. *Mol. Med*. 21:526–35.